A Proportional + Multi-Resonant Current Controller for Grid-connected Inverters under Unbalanced Grid Voltage

Jiajin Pan[a], Yancheng Liu[b], Qinjin Zhang[c] , Ning Wang[d]

Marine Engineering College, Dalian Maritime University, Dalian, 116026, China

[a]ballfrank@163.com, [b]liuyc3@126.com, [c]zqj18@qq.com, [d]n.wang.dmu.cn@gmail.com

Keywords: grid voltage unbalance and distortion; proportion multi-resonant (PMR); second order generalized integrator (SOGI); zero current error control

Abstract. The traditional grid-connected inverter (GCI) has the disadvantage of high total harmonic distortion under the condition of unbalanced and distorted grid voltage. On this basis, a novel GCI control strategy is proposed in this paper. Firstly, a second order generalized integrator is built in the *αβ* coordinate to realize the grid voltage phase shift 90° and separate the positive-and negative -sequence. Then, the grid current reference command of the GCI is derived. Secondly, a proportional + multi-resonant (PMR) controller, which does not need positive-and negative - sequence separation of the grid current, is employed to achieve zero current error control and improve the grid current power quality. Finally, simulation results demonstrate the effectiveness of the proposed scheme under the condition of unbalanced and distorted grid voltage.

Introduction

Energy shortage and environmental pollution are the major problems that affect the world today. With the advantage of zero emissions, low pollution, and low price, solar energy has become the focus of all countries [1, 2]. As one of the most important parts in photovoltaic generation system, GCI provides more technical benefits and control flexibilities to the utility. When the grid voltage is unbalanced and distorted, the traditional control method cannot operate stably because of the existing of positive-and negative-sequence components. Due to a lack of control ability to the negative sequence component, the traditional control method would result in twice frequency fluctuations of the active and reactive power. Accordingly, study of the GCI control strategy under unbalanced and distorted grid voltage has practical significance [3, 4].

A feed-forward control strategy based on positive *dq* frame is used to improve the output current of GCI [5, 6]. The unbalanced grid information is added into the controller. The control effort of this method is very well when the unbalanced factor is small, whereas its control effort is serious when the unbalanced factor is large. In Ref. [7], the positive-and negative-sequence components of the grid-current are controlled respectively by the PI regulator in the positive and negative sequence *dq* frame. However, this method would result in delay and error because of the positive-and negative-sequence separation of the grid current. Ref. [8] adopts a proportional integrator resonant (PI-R) controller in the positive *dq* frame to track the reference current of the three-phase GCI system during grid voltage distortion. However, this method needs complex coordinate transformation.

An improved strategy for GCI under distorted and unbalanced grid voltage is proposed in this paper. The positive-and negative sequence grid voltages in *αβ* frame are detected by using SOGI. On the basis, the proportional + multi-resonant (PMR) controller, which is composed of the traditional proportional resonant (PR) controller and the harmonic resonant controllers of 3^{th}, 5^{th}, and 7^{th}, is used to realize the unbalance control targets. This method can effectively restrain the grid current influence of the grid voltage distortion. Finally, the effectiveness of the proposed control scheme is evaluated by the simulation results.

Topology of GCI under Unbalanced Grid Voltage

The schematic diagram of a typical GCI is shown in Fig.1. A standard three-phase GCI is connected to the grid through a filter. U_{dc} is the DC bus voltage , i_i (i = a, b, c) is the current of the output of GCI, u_{gi} (i = a, b, c) is the grid voltage, L_1, L_2, and C are the filter inductance and capacitor, R is the reactive damping resistor that is used to inhibit the damping of LCL filter [9].

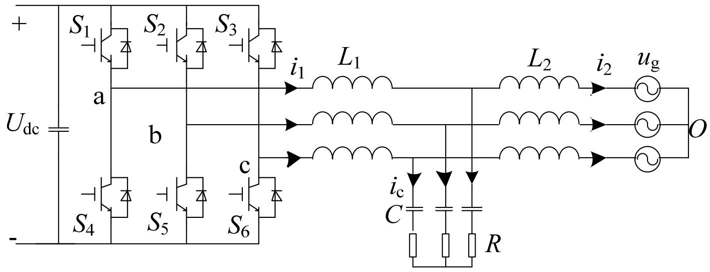

Fig.1 The schematic diagram of a typical GCI.

SOGI. Due to the existence of the positive-and negative-sequence components under the grid voltage unbalanced, the control effect is not ideal; therefore, it is necessary to separate the two components to achieve the current unbalanced control [10]. In this paper, the SOGI is constructed to shift the grid voltage phase 90°, so positive-and negative-sequence components can be separated. The structure of the SOGI is shown in Fig. 2.

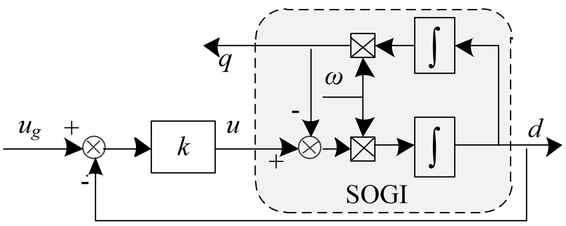

Fig. 2 The structure of the SOGI.

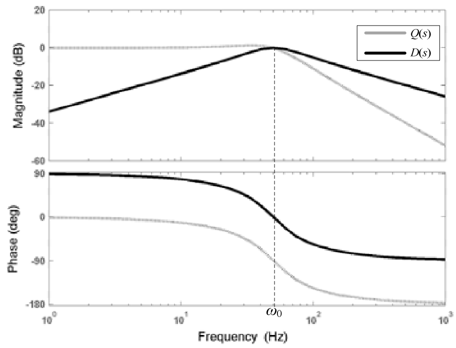

Fig. 3 Bode diagram of $D(s)$ and $Q(s)$.

The two in-quadrature output signals of the SOGI in Fig. 2, i.e., d and q, are defined by the following transfer functions:

$$D(s) = \frac{d(s)}{u_g(s)} = \frac{k\omega s}{s^2 + k\omega s + \omega^2} \tag{1}$$

$$Q(s) = \frac{q(s)}{u_g(s)} = \frac{k\omega^2}{s^2 + k\omega s + \omega^2} \tag{2}$$

Where k is damping ratio, ω is the angular frequency of fundamental wave.

The bode diagrams of D(s) and Q(s) when k=1 are shown in Fig. 3. It can be concluded that the output of Q(s) is always 90° lagged from D(s). Moreover, when the angular frequency is ω_0， the magnitude of D(s) and Q(s) is zero. It shows that the magnitudes of input and output of SOGI are nearly the same.

Positive-and Negative-Sequence Separation. According to the instantaneous symmetrical components method, the positive-and negative-sequence components of grid voltage can be described as follows:

$$u_{abc}^{+} = \begin{bmatrix} u_a^+ \\ u_b^+ \\ u_c^+ \end{bmatrix} = \frac{1}{3}\begin{bmatrix} 1 & a & a^2 \\ a^2 & 1 & a \\ a & a^2 & 1 \end{bmatrix}\begin{bmatrix} u_a \\ u_b \\ u_c \end{bmatrix} = \boldsymbol{T}_{+} u_{abc} \tag{3}$$

$$u_{\text{abc}}^{-}=\begin{bmatrix}u_{\text{a}}^{-}\\u_{\text{b}}^{-}\\u_{\text{c}}^{-}\end{bmatrix}=\frac{1}{3}\begin{bmatrix}1 & a^2 & a\\a & 1 & a^2\\a^2 & a & 1\end{bmatrix}\begin{bmatrix}u_{\text{a}}\\u_{\text{b}}\\u_{\text{c}}\end{bmatrix}=\boldsymbol{T}_{-}u_{\text{abc}} \tag{4}$$

where, $a=\mathbf{e}^{j120°}=-\frac{1}{2}+j\frac{\sqrt{3}}{2}$, u_{a}, u_{b}, and u_{c} are the three-phase voltages, u_a^+, u_b^+, and u_c^+ are the positive-sequence components, u_a^-, u_b^-, and u_c^- are the negative-sequence components.

The positive-and negative-sequence components of instantaneous voltage in the $\alpha\beta$ frame, which transformed from the abc frame by using *Clarke* transformation, can be calculated as shown in Eqs. 5 and 6.

$$u_{\alpha\beta}^{+}=\boldsymbol{T}_{\alpha\beta}u_{\text{abc}}^{+}=\boldsymbol{T}_{\alpha\beta}\boldsymbol{T}_{+}u_{\text{abc}}=\boldsymbol{T}_{\alpha\beta}\boldsymbol{T}_{+}\boldsymbol{T}_{\alpha\beta}^{-}u_{\alpha\beta}=\frac{1}{2}\begin{bmatrix}1 & -S\\S & 1\end{bmatrix}u_{\alpha\beta} \tag{5}$$

$$u_{\alpha\beta}^{-}=\boldsymbol{T}_{\alpha\beta}u_{\text{abc}}^{-}=\boldsymbol{T}_{\alpha\beta}\boldsymbol{T}_{-}u_{\text{abc}}=\boldsymbol{T}_{\alpha\beta}\boldsymbol{T}_{-}\boldsymbol{T}_{\alpha\beta}^{-}u_{\alpha\beta}=\frac{1}{2}\begin{bmatrix}1 & S\\-S & 1\end{bmatrix}u_{\alpha\beta} \tag{6}$$

where, $\boldsymbol{T}_{\alpha\beta}$ is the array of *Clarke* transformation, $\boldsymbol{T}_{\alpha\beta}^{-}$ is the array of *anti-Clarke* transformation, $S=\mathbf{e}^{-j90°}$ is a 90° lagging phase-shifting operator.

According to the analyses above, the principle diagram of positive and negative sequence separation is obtained as Fig. 4.

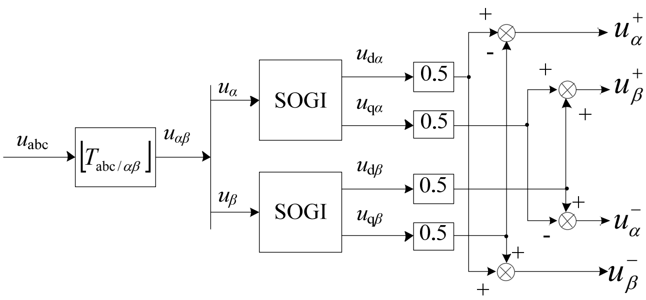

Fig. 4 Principle of positive and negative sequence detection.

Controller Design

Once the positive-and negative-sequence of grid voltage and referenced current are determined, the next task is to design the grid controller to ensure that the grid current can follow the referenced signal. Then the PMR controller is adopted in this paper.

PMR controller. The PMR transfer function is defined as follows:

$$G_{\text{PMR}}(s)=k_{\text{p}}+\sum_{\text{m}=1,3,5,7}\frac{2k_{\text{r}}m\xi_0\omega_0 s}{s^2+2m\xi_0\omega_0 s+(m\omega_0)^2} \tag{7}$$

where, k_{p} is the proportional coefficient and k_{r} is the multi-resonant coefficient, ω_0 is the fundamental frequency and its value is 100π rad/s, ξ_0 is the resonant factor.

As shown in Fig.5, the resonant peaks are existed in the frequency of $m\omega_0$; therefore, the system will have great gains in these frequencies and the zero-error tracking for the referenced current can be realized.

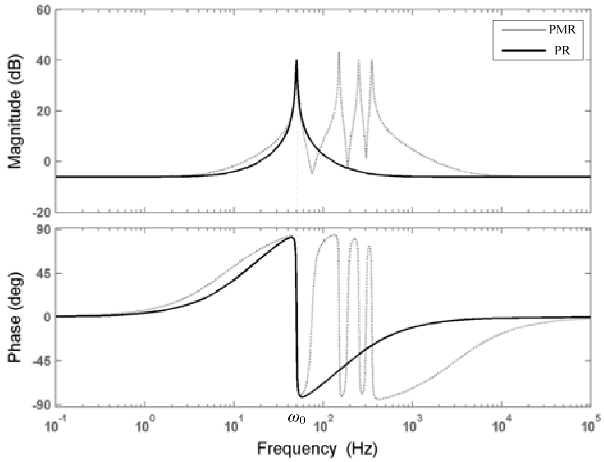

Fig. 5 Bode diagram of PR and PMR.

It can be seen from Fig.5 that, the resonance peak is existed only in the fundamental frequency when PR controller is used; therefore, the controller cannot achieve the current zero-error control and get ideal control effect when the grid voltage contains multiple harmonics.

Grid-connection control strategy. According to the principle of control strategy [3], the grid current control system of GCI under unbalanced grid voltage can be designed. The structure of grid-connection control strategy is shown in Fig. 6

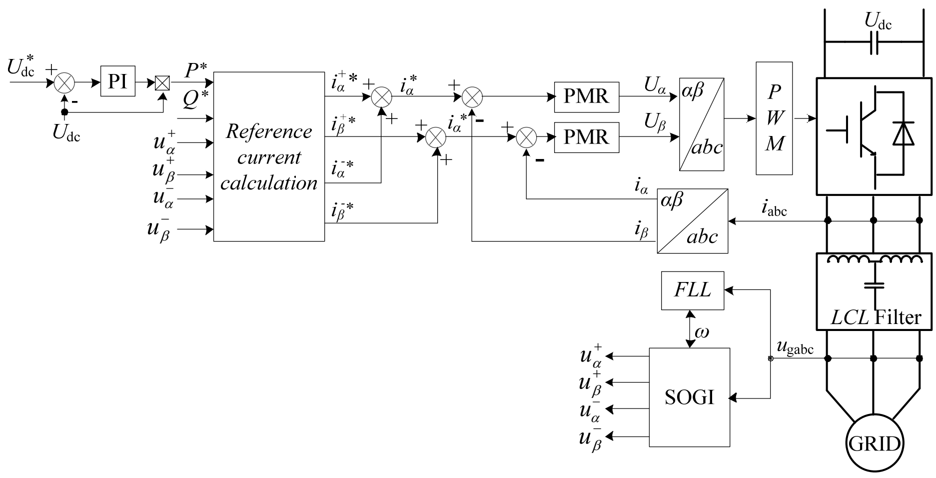

Fig. 6 Structure of the GCI control strategy.

The grid-connection control strategy is composed of DC voltage outer loop and PMR current inner loop. The outer loop provides the active power reference command to the inner loop, while the inner loop tracks the given current and eliminates the certain harmonics; thus the grid current power quality can be improved.

Firstly, the phase, frequency, and amplitude of grid voltage are detected, and its positive-and negative-sequence components are separated by the positive-and negative-sequence separation module in αβ frame. Then the referenced current command is calculated by combining with output of outer loop. The error between the referenced current command and actual grid current is then sent to the PMR controller to get high quality of grid current.

As shown in Fig. 6, the proposed control system does not need to separate the positive- and negative-sequence currents and it is designed in stationary frame. The PMR regulator can realize the precise control of negative-sequence current, and ensure the system dynamic response.

Simulation Results

In order to verify the effectiveness of the proposed control strategy, the control system was simulated using matlab/simulink. Unbalanced grid voltage condition is used in the simulation. In order to compare the PMR control strategy with the traditional method, Fig. 7 shows the grid currents and total harmonic distortion (THD) of the GCI under the two control method, the grid voltage is unbalanced and with 3th, 5th and 7th harmonics.

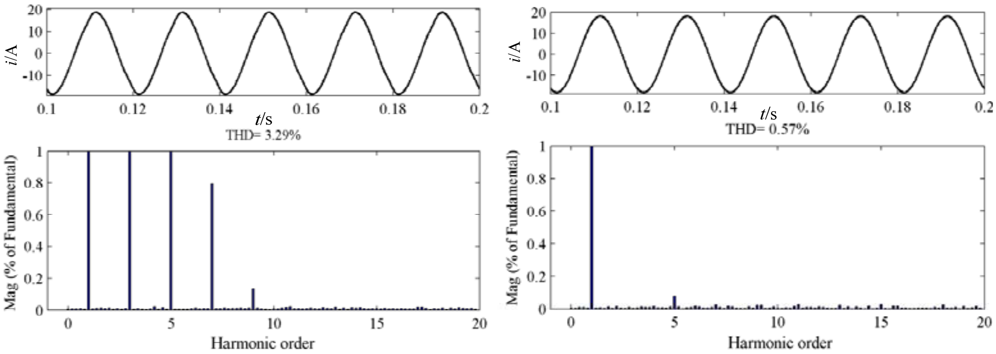

(a) (b)

Fig. 7 Grid-current waveform and THD: (a) traditional control scheme, (b) the proposed scheme.

It can be seen from the simulation results that the output grid-current has a good performance and a low THD under the proposed control scheme, especially in 3th, 5th and 7th harmonic sequences of the GCI

Fig. 8(a) shows the active and reactive power under unbalanced grid voltage. The active power is constant and the reactive is zero. It can be seen that the two-times frequency fluctuation of active power can be effectively suppressed under the proposed control strategy.

Fig. 8(b) shows the reference current i^* and detected grid current i in $\alpha\beta$ frame. It shows that the control scheme can achieve zero current error control.

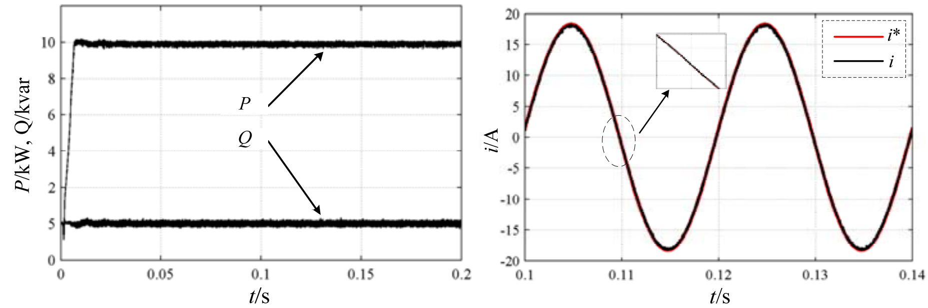

(a) (b)

Fig. 8 Simulation of GCI: (a) active and reactive power, (b) reference current and grid current.

Summary

An advanced control scheme, which is composed of SOGI and PMR regulator, is proposed for the GCI under unbalanced grid voltage in this paper. The SOGI is constructed to realize the grid voltage phase shift 90°. Due to the lack of the grid synchronous rotation angle extraction, the delay of low pass filter can be reduced and the system dynamic performance can be improved. The PMR regulator can effectively eliminate the 3th, 5th and 7th harmonic sequences and obtain a good dynamic performance, it needs not to calculate the positive-and negative-sequence grid-currents, so the design of the control strategy is simplified. Simulation validates the effectiveness of the proposed control strategy.

Acknowledgements

This work is supported by the National Natural Science Foundation of P.R. China (under Grants 51479018, 51379002), Program for Liaoning Excellent Talents in University (under Grant LJQ2013055), and Fundamental Research Funds for the Central Universities of P.R. China (under Grants 313201432).

References

[1] Z. Zhao, M. Xu, and Q.L. Chen, *et al*. Derivation, Analysis, and Implementation of a Boost–Buck Converter-Based High-Efficiency PV Inverter [J]. *IEEE Tran. Power. Electron*. , vol. 27, no. 3, pp. 1304-1312, Mar. 2012.

[2] R. A. Mastromauro, M. Liserre, and A. D. Aquila. Control Issues in Single-Stage Photovoltaic Systems: MPPT, Current and Voltage Control [J]. *IEEE Tran. Ind. Inform*. , vol. 8, no. 2, pp. 241-253, May 2012.

[3] M. Castilla, J. Miret, and A. Camacho, *et al*. Voltage Support Control Strategies for Static Synchronous Compensators under Unbalanced Voltage Sags [J]. *IEEE Tran. Ind. Electron*. , vol. 61, no. 2, pp. 808-819, Feb. 2014.

[4] J. B. Hu, and Y. K. He. Modeling and Control of Grid-Connected Voltage-Sourced Converters under Generalized Unbalanced Operation Conditions [J]. *IEEE Tran. Energy Con*., vol. 23, no. 3, pp. 903-913, Sep. 2008.

[5] D. Vincenti, and H. Jin. A Three-phase Regulated PWM Rectifier with On-Line Feed-forward Input Unbalance Correction [J]. *IEEE Tran. Ind. Electron*. , vol. 41, no. 5, pp. 526-532, Oct. 1994.

[6] P. Rioual, H. Pouliquen, and J.P. Louis. Regulation of a PWM Rectifier in the Unbalanced Network State Using a Generalized Model [J]. *IEEE Tran*. *Power*. *Electron*. , vol. 11, no. 3, pp. 495-502, May. 1996.

[7] H. Song, and K. Nam. Dual Current Control Scheme for PWM Converter under Unbalanced Input Voltage Conditions [J]. *IEEE Tran. Ind. Electron.* , vol. 46, no. 5, pp. 953-959, Oct. 1999.

[8] J. B. Hu, Y. K. He, and L. Xu, *et al.* Improved Control of DFIG Systems During Network Unbalance Using PI–R Current Regulators [J]. *IEEE Tran. Ind. Electron.* , vol. 56, no. 2, pp. 439-450, Feb. 2009.

[9] D. S. Yang, X. B. Ruan, and H. Wu. Impedance Shaping of the Grid-Connected Inverter with LCL Filter to Improve Its Adaptability to the Weak Grid Condition [J]. *IEEE Tran. Power. Electron.* , vol. 29, no. 11, pp. 5795-5804, Nov. 2014.

[10] P. Rodríguez, A. Luna, and I. Candela. Multiresonant Frequency-Locked Loop for Grid Synchronization of Power Converters Under Distorted Grid Conditions [J]. *IEEE Tran. Ind. Electron.* , vol. 58, no. 1, pp. 127-138, Jan. 2011.